MULTI-SENSOR PERSONAL NAVIGATOR SUPPORTED BY HUMAN MOTION DYNAMICS MODEL

Dorota A. Grejner-Brzezinska, Charles Toth, Shahram Moafipoor and Yoonseok Jwa
Satellite Positioning and Inertial Navigation (SPIN) Lab
The Ohio State University
dbrzezinska@osu.edu

Jay Kwon
Dept. of Geoinformatics, University of Seoul
Seoul, Korea

Abstract: This paper presents preliminary results of a prototype design and implementation of a multi-sensor personal navigator suitable for navigation in open areas and confined environments. This work, supported by the National Geospatial-Intelligence Agency (NGA), is focused on forming theoretical foundations for such a system by developing the algorithmic concept of a basic GPS-based, Micro-electro-mechanical inertial measurement unit (MEMS IMU)-augmented personal navigator system with an open-ended architecture, which would be able to incorporate additional navigation and imaging sensor data, extending the system's operations to indoor environments. The accuracy requirement is considered at 3-5 m CEP (circular error probable). In the current system design and implementation, the following sensors are integrated in the tightly coupled Extended Kalman Filter: GPS pseudoranges, Crossbow IMU400C, PTB220A barometer and Azimuth 1000 digital compass.

In order to bridge GPS signal gaps in impeded environments, the dynamic model of human locomotion is currently included in the system architecture. The system is trained under the open sky conditions, where GPS signals are available, and is subsequently used to support navigation when GPS signals are obstructed. The calibrated model of stride length and stride interval extracted from the test data provided by GPS/IMU, and heading information from compass and IMU offer dead reckoning navigation, facilitating bridging of GPS gaps.

1. Introduction

Accurate and reliable navigation and tracking is a necessity for ground personnel in combat and emergency situations. Protecting ground troops while maintaining combat or rescue operation effectiveness requires precise individual geolocation of all military and emergency personnel in real time. Assuming the availability of two-way communication between the troops or the emergency crews and the command center, personal navigators would ideally assure that ground personnel can execute their tasks in an optimal way, without unnecessary risk exposure. Since the early 1990s, the Global Positioning System (GPS) has become the primary navigation and tracking technology for airborne and land military vehicles, and, recently, also for dispatching and guiding emergency response vehicles and crews. However, GPS is a line-of-sight system and is also subject to jamming and interference; thus signal coverage and continuity are not always guaranteed. The effectiveness of GPS can be significantly reduced in urban scenarios where most

military or rescue operations take place. Consequently, some form of GPS augmentation is needed.

With GPS currently undergoing modernization, and micro-elector-mechanical (MEMS) inertial measurement unit (IMU) technology steadily improving and becoming more affordable, with the target of achieving 1°/h gyro stability in the next few years, it seems logical to consider these sensors as primary technology components for the future personal navigator. This research aims at forming the theoretical foundations for such systems by developing the algorithmic concept of a basic GPS-based, MEMS IMU-augmented personal navigation system with an open-ended architecture, which would be able to incorporate additional navigation and imaging sensor data, extending the system's operations to indoor environments. While a variety of sensors and their integration algorithms have been available for a number of years, what is lacking at the moment is the availability of techniques, methods and their software implementation that may exploit the potential of combining highly portable versions of these sensors into seamless and dependable hand-held devices. Therefore, using sensor fusion technology, the proposed research is directed towards prototyping a portable navigation sensor suite with the necessary processing techniques to provide seamless navigation and tracking of the ground personnel under various situations where GPS signal reception is not always guaranteed, such as urban canyons, under canopy or inside buildings.

In the context of the research presented here, the positioning errors related to the duration of GPS signal blockage, and the quality of the IMU sensors and the supporting instrumentation, such as digital compass and the barometer, are of great interest. As far as the navigation errors are concerned, the primary interest will be in determining the real capabilities of the MEMS IMU sensors by testing and simulations.

In order to achieve optimal design and performance characteristics, as well as seamless real-time navigation operations, our research focuses on (1) the selection of the most suitable sensor performance parameters ensuring redundancy and complementarity, (2) the investigation of the optimal filtering approach for real-time navigation, and (3) extensive testing in real world scenarios.

2. Multi-sensor System Design, Sensor Selection and Navigation Data Types

Figures 1 a-b show a conceptual design of the multi-senor system implemented in the tightly coupled Extended Kalman Filter (EKF) architecture, and Table 1 provides the corresponding stochastic error models used in the current implementation. The GPS measurements used currently are double-differenced carrier phase and/or pseudorange data at 1Hz; dual frequency receiver, Novatel OEM-4, is used in the current prototype. Other hardware components include Crossbow MEMS IMU400C (see Table 2), PTB220A barometer (500–1100hPa pressure range, -40–140F temperature range, 0.5–10Hz update rate, 0.1–3s output averaging time, and 1.5 m height accuracy (1 σ)) and KVH Azimuth 1000 digital compass ($\pm$25°gimbal rate, 10 Hz read-out rate, and $\pm$1.1° heading accuracy). A NAVSYNC GPS Receiver CW25 Development Kit (http://www.navsync.com/GPS_Receiver_Chipset1.html) is currently considered for implementation in the multi-sensor navigator prototype.

The proposed selection of the sensors is driven mainly by size and cost factors. While the accuracy of each sensor and the interface type are critical factors for the proposed sensor fusion, the currently achievable performance of some portable sensors might still not be fully adequate for our target application. Thus, based on the primary objective of this research, preference is given to simple sensors that can be easily integrated into a light hand-held navigation device, with the understanding that the "ideal" sensor performance will be simulated. For possible long-term outages of GPS signals, a heading compensation by the KVH Azimuth 1000 sensor would be necessary, as the dominant error in inertial orientation comes from heading. The hardware composition and the software design are motivated by practicality – the device must be simple and versatile for individual personnel use. Also, by considering the expected future individual sensor performance that will be simulated to reflect the expected system prototype based on the state-of-the-art technology, as well as offering the open-ended architecture that facilities an easy expansion of the sensor suite.

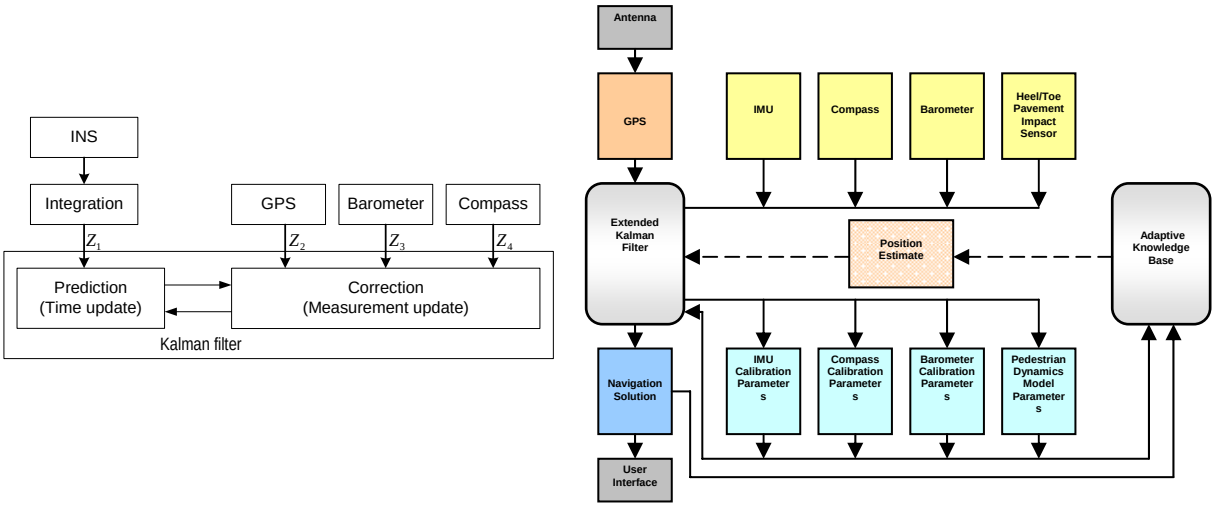

Figure 1: Conceptual design of the integrated filter, Z_i (i = 1, 2, 3, 4) indicate multi-senor measurements (a); conceptual design of the multi-sensor integrated system (b).

Precise timing of all the sensory data to GPS time is essential for sensor integration. For more sophisticated use, the GPS time must be externally recovered from the 1PPS signal, available through standard interface from a GPS receiver. This solution requires timer hardware and control software. The disadvantage of the extra hardware is well offset by the flexibility offered by the excellent time-tagging capabilities of the GPS-clock-synchronized external timing system. For this system, a timer board is used, whose main advantage is the accurate time-tagging of various sensory data. Furthermore, this solution allows for a thorough analysis of the clock subsystems of the different sensors, including drift, absolute accuracy and temperature dependency, etc. The selected board, model PCI-CTR05 from Measurement Computing, has a PCI interface with drivers for major operating systems.

The primary data types that are used are the GPS pseudorange observations, the raw accelerometer and gyroscope data, and the heading (yaw) measurements from the digital compass, as well as the height information from the barometer. In the calibration stage,

also carrier phase data are used. The height information is important to include, especially during GPS outages, as during the free inertial navigation the vertical channel drifts the most. Receiving differential corrections is considered; however, a stand alone positioning algorithm (no reference base or differential corrections) will most probably be preferred.

Sensor	Error sources	Stochastic error model
Accelerometer	Bias	Random walk
	Scale factor	Random constant
Gyroscope	Bias	Random walk
	Scale factor	Random constant
Barometer	Bias	Random walk
Digital Compass	Bias	1st GMM

Table 1: Stochastic error models for multi-sensor error sources;
GMM stands for Gauss-Markov Model.

It should be pointed out that the open-ended architecture will allow for including pseudolite observable as an alternative and/or augmentation to the GPS signals. A portable, deployable network of pseudolites, such as Locata Lites [1], should be considered an option for future combat and emergency situations, as this technology evolves. In addition, the flexible architecture of the navigation filter, as described next, will allow for an easy extension of the processing algorithms to include direct feedback from the (optional) imaging component that might be added in the future.

IMU Error	Acceleration Bias	8.5 mg	Random walk	Velocity	0.1 m/s/$\sqrt{hr}$
	Acceleration Scale Factor	1%		Attitude	2.25 °/$\sqrt{h}$
		1.0e-2		Acceleration Bias	0.05 m/s/$\sqrt{h}$
	Gyro Bias	1 °/s		Acceleration Scale Factor	0.0
	Gyro Scale Factor	1 %		Gyro Bias	0.85 °/$\sqrt{h}$
		1.0e-2			

Table 2: IMU400C error specifications.

3. Preliminary Performance Analysis

The initial performance tests were conducted at the OSU Campus in July-November 2005. During these trials, GPS, IMU, compass and barometer data were collected. In the performance analyses presented here, these and simulated data were used. First part of the analyses presented in the next section is based on synthetic data used for checking the performance of the hardware components, to assess their relevance to the accuracy specs of the system. The actual data collected during the tests discussed here were GPS and LN100, while other sensor data were simulated using the manufacturer specifications for their error characteristics.

3.1 Navigation Accuracy of GPS/IMU/Compass/Barometer Sensor Assembly

In order to assess the accuracy achieved with pseudorange data, the pseudorange/MEMS IMU (simulated) positioning results were compared to the reference solution, i.e., carrier phase/LN100 (0.8 nmi/h CEP, gyro bias – 0.003°/h, accelerometer bias – 25μg), and subsequently compass and barometer data (simulated) were added to test their impact, as shown in Table 3. Figure 2 illustrates the impact of barometer and compass data on the accuracy of the pseudorange solution. Table 4 describes the parameters of the solutions illustrated in Figure 2 and Table 3. A total of 15 minutes of simulated data were used. The reference solution is based on the OSU AIMS™ system (see, for example, [2]).

	Reference-solution 1		Reference-solution 2	
	Mean	STD	Mean	STD
N [m]	0.66	0.54	0.58	0. 50
E [m]	0.80	0.69	0.72	0.58
U [m]	0.93	0.71	0.80	0.53
Roll [°]	1.38	0.95	1.36	1.00
Pitch [°]	1.47	0.96	1.00	0.78
Heading [°]	10.68	8.46	1.05	0.78

Table 3: Position and attitude mean error and STD of the pseudorange/MEMS IMU model (solution 1) and the pseudorange/MEMS IMU/compass/barometer model (solution 2) with respect to the reference solution (carrier phase/LN100).

Solution #	Description
C	Reference solution with dual-frequency carrier phase + LN100 INS
P	pseudorange + simulated MEMS IMU measurements
Cbc	solution P + Barometer + Compass measurements

Table 4: Solution reference.

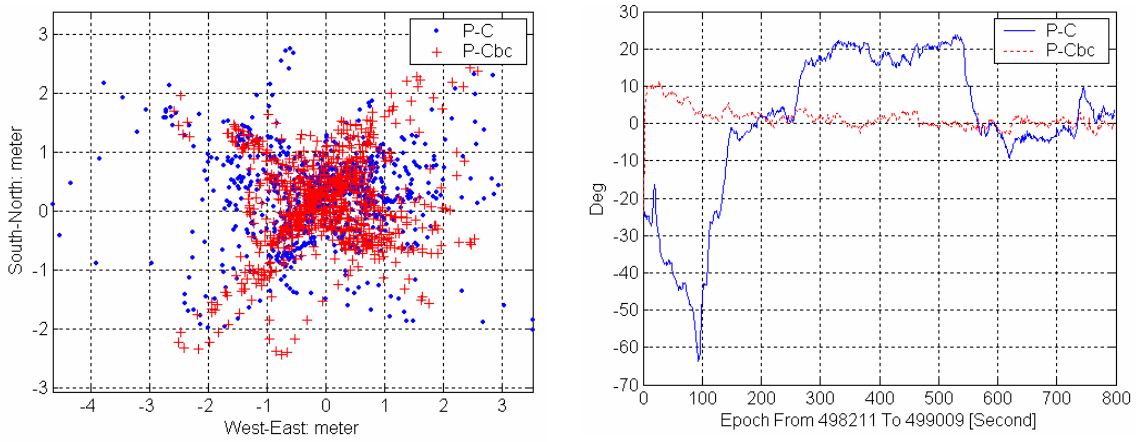

Figure 2: Positioning accuracy (left) and heading accuracy (right) of the solutions listed in Table 7 with respect to carrier-phase reference solution (P).

As can be observed in Table 3, the barometer improves the height accuracy, but the most pronounced improvement is evident in heading, as a result of including the compass measurements. Table 5 illustrates the position and attitude error performance of solutions 1 and 2 during GPS gaps. As expected, the stand-alone IMU provides the largest drift in most of the position and attitude solutions, and the errors grow with the gap duration. The heading error is very significant, even after the shortest gap; thus, the low-cost inertial sensor, like the MEMS IMU tested here, may not be adequate for our application. In case of the IMU integrated with the barometer and compass, heading and height values are improved. There is also some small improvement in other states (not directly observed by the compass or barometer), primarily due to the state correlation. In general, GPS/IMU with barometer and compass may be sufficient for a personal navigator in indoor as well as outdoor environments, but the IMU sensor must be of better quality (for example, a tactical grade gyro ~1-5 °/hour bias stability should be sufficient).

		30sec		120sec			30sec		120sec	
		Mean	Std	Mean	Std		Mean	Std	Mean	Std
IMU Only	N [m]	66.9	79.0	2472.7	3288.9	R [°]	4.1	4.6	6.6	8.2
	E [m]	334.6	456.0	6542.0	8910.6	P [°]	9.3	10.6	16.5	19.0
	U [m]	72.1	93.0	1331.4	1857.5	H [°]	125.6	143.3	184.3	215.0
IMU +Barometer +Compass	N [m]	476.7	616.9	3038.4	3731.9	R [°]	4.1	4.8	5.0	6.1
	E [m]	93.8	142.3	673.3	787.5	P [°]	6.8	8.3	10.2	12.5
	U [m]	11.3	11.9	4.8	6.3	H [°]	0.5	0.7	0.5	0.5

Table 5: Position and attitude error during GPS gaps.

3.2 Barometer and Compass Performance Testing

The digital compass was tested in kinematic environment, as presented next. During the straight course of the trajectory shown in Figure 3, the mean difference between the reference solution and the compass reading was 1.11°. Since the compass was compensated for declination, this difference can be considered as sensor-dependent bias introduced by the magnetic disturbance. Heading analysis during turning movements showed some delay of the value generated by the magnetic compass with respect to the one estimated by the reference solution. The mean difference with respect to the reference solution was estimated at ~4.9°. Figure 4 shows an example of the empirically found delay of the compass measurement, by about 5 ~ 6 seconds, w.r.t. the reference navigation solution. This indicates that an access to raw compass data is desired, as a possibility of the internal over-smoothing exists. Tuning the compass raw readings against a reference heading would allow selection of the necessary level of internal smoothing that would not be detrimental to the navigation requirements of this project. This issue is currently under investigation.

As indicated earlier, compass bias is also estimated in the integrated filter when GPS is available (and thus, corrected heading from the calibrated IMU is also available). After the bias compensation, the compass heading shows a very good agreement with the reference heading, as shown in Table 6 and Figure 5. However, the compass bias itself is a function of the trajectory dynamics/surrounding environment, thus more investigation is currently carried out on the applicability of the estimated bias to the portions of the

trajectory during the GPS signal blockage (see also section 4). It should be noted that the test data analyzed in the next section did not display significant dynamics, so no considerable compass delay with respect to the actual motion was observed.

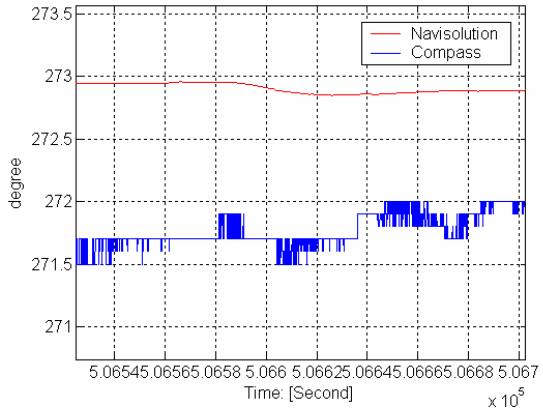

Figure 3: Compass and reference heading after declination compensation: straight trajectory (top) and varying dynamics trajectory (bottom).

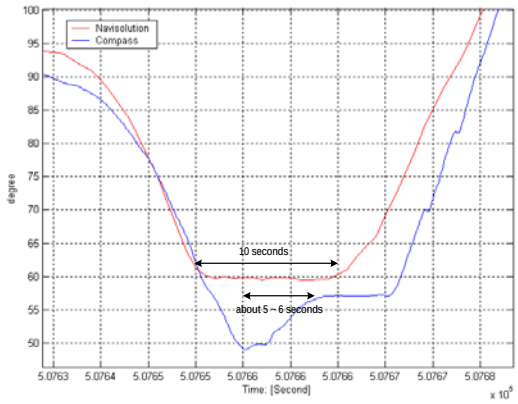

Figure 4: The delay of the compass measurement w.r.t. the actual heading change.

Straight course		Turning movements	
Mean [deg]	STD [deg]	Mean [deg]	STD [deg]
0.15	0.01	0.15	0.12

Table 6: Mean and STD of differences between the reference and compass heading after compass error compensation.

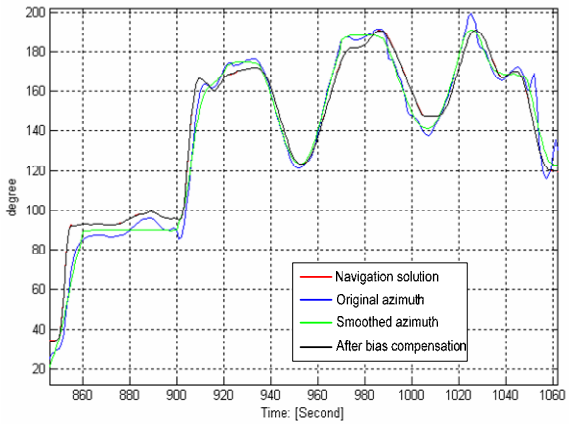

Figure 5: Original heading (compass), compass heading after the delay effect removal (smoothed), reference solution (GPS/LN100) and heading after compass bias compensation.

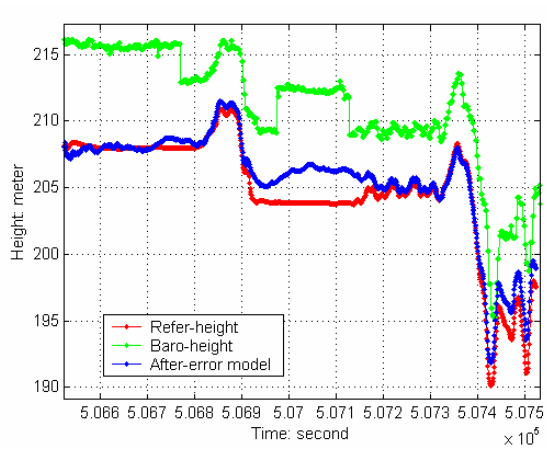

Figure 6: Difference between the reference height and the barometric height before and after the error model compensation.

Another aspect that should be noted is a limited gimbal range for the Azimuth 1000 sensor (±25°). In general, larger departures from horizontal orientation may happen in personal navigation, thus, additional calibration may be needed. However, due to the over-smoothing problems already mentioned, an alternative sensor is now under consideration; KVH C100 seems to be a good candidate, as one can select totally un-damped output, and handle signal filtering internally. It is also much smaller than Azimuth 1000, which is important to the system's portability.

In order to obtain an averaged pressure reading from PTB22A barometer, the averaging time should be selected. This barometer provides the averaging time from 1 to 600 seconds. The averaging times of 1, 2, 3, 5, 10, and 30 seconds were tested, with 60 measurements in each sample. All other conditions were the same. The standard deviation of the barometer observations as a function of the averaging time indicates that 2- and 3-second averaging times show the smallest STD of 10 cm, while longer averaging times increase the STD to 34 cm. As mentioned earlier, a bias for the barometer is estimated in the EKF during the GPS signal availability. An example of the effect of bias compensation is presented in Figure 6.

4. Navigation during GPS Loss of Lock

Pedestrian navigation supported by human body dynamics (locomotion) model has been studied earlier (e.g., [3]; [4]; [5]). In most cases, the stride frequency and interval were determined by analyzing the spectrum of the acceleration signal provided by an IMU. This can be a tedious process, requiring extensive testing for threshold selection on a case-by-case basis. In this implementation, an additional sensor, an impact switch, is added to directly measure the events of foot-to-ground impact, synchronized to GPS time. The research on integrating the switch events is currently under way, and will be reported in details in the upcoming publication. A few preliminary results are shown here.

In general, a known (estimated) human locomotion model can be used to support navigation during GPS gaps, meaning that (at the minimum) the step interval (frequency) and length must be pre-calibrated, and heading information from compass/IMU should be available. The system must be trained during the GPS signal availability, and the training must be customized for a particular user. Therefore, a learning mechanism, generally outside the positioning filter, must be designed and implemented, to assure a proper calibration/training procedure that would support reliable navigation without GPS (see, Figure 1). Fuzzy logic or neural network methods are currently considered for this project (e.g., [6]; [7]). It should be mentioned that sensor configuration and location on the user's body are also important factors, and cannot be overlooked in the calibration procedure. In the preliminary results presented here backpack configuration was used, but this is not the final sensor configuration for that system.

The step length is defined here as the distance between the left and right heel sensors, and it was extracted for a specific user moving on a flat circular path, as shown in Figure 7 (three repetitions of the same circular motion pattern were used here). Double difference carrier phase data were used to calibrate the step length for the events measured by the impact switches.

In order to test the step calibration results, GPS signal was turned off for one loop, and the navigation was performed using the compass heading (calibrated during the previous loop), the step size presented in Table 7 (loop 2, operator A), rescaled to 1/second sampling, and the step frequency (events) sensed by the impact switches. The navigation results compared to the correct (GPS) trajectory are presented in Figure 7. The final closure in the end of the loop is 3.22 m (Figure 7, left), which is well within the required accuracy specifications. If varying step size is used, according to the dynamics along the trajectory, better results are obtained, as shown in Figure 7, right. The next step is to test the calibration procedure along the trajectory with a varying height.

Step Length	Operator A		Operator B	
	Mean [m]	Std [m]	Mean [m]	Std [m]
Loop 1	0.61	0.05	0.67	0.06
Loop 2	0.63	0.04	0.64	0.09
Loop 3	0.72	0.10	0.72	0.09

Table 7: Mean and STD of step length determined from three trials for two operators.

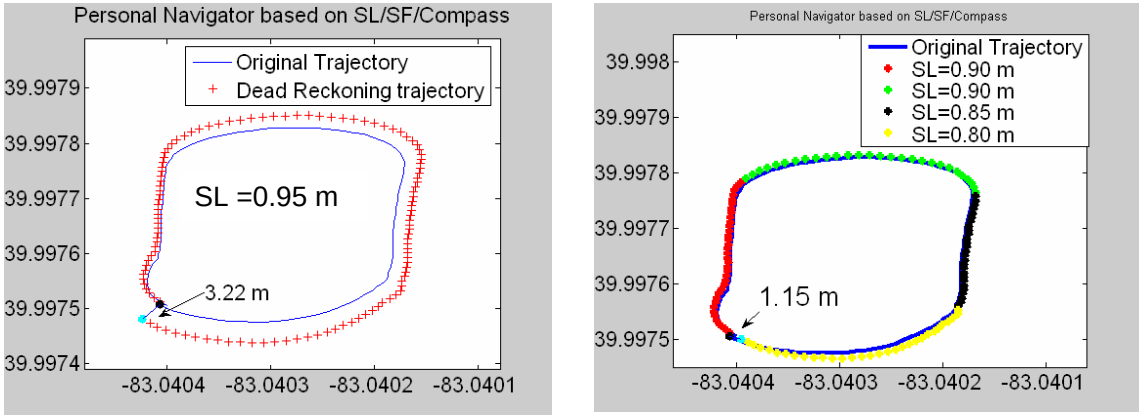

Figure 7: Reference and predicted trajectories; prediction is based on calibrated compass and step size/frequency data; left – single step length used, right – several step-length (SL) used depending on trajectory dynamics.

5. Summary and Conclusions

A preliminary implementation of a multi-sensor personal navigator was presented. Simulation-based performance analyses for IMU, digital compass and barometer were disused, and a multi-sensor navigation performance was tested in the actual kinematic scenario, with a special emphasis on the accuracy of the navigation supported by the pre-calibrated simple human dynamics model (i.e., single step length and frequency were used). The preliminary results are encouraging; however, the currently used MEMS IMU 400CC may not be the desirable sensor, as its gyro drifts very fast, and may not be able to provide the required accuracy and stability to the orientation solution. More detailed study of this sensor is presented in [8] and [9]. The human dynamics-supported navigation, tested with real kinematic data, especially with the impact switches that we use to detect the step events, is very promising. With this solution, no spectral analyses of

the acceleration are needed to detect the step frequency. More tests are currently carried out to test the accuracy of navigation for varying step length along the trajectory and for more complicated trajectories, with varying vertical component.

Acknowledgement

This project is sponsored by the National Geospatial-Intelligence Agency (NGA) 2004 NURI Grant.

References

[1] Barnes J., Rizos C., Wang J., Small D., Voigt G. and Gambale N.: Locata: the positioning technology of the future?, Proceedings of SatNav 2003, The 6th International Symposium on Mobile Positioning and Location Services, Melbourne, Australia, 22-25 July, paper 49, CD ROM, 2003.

[2] Toth C., Grejner-Brzezinska, D. A.: Performance Analysis of the Airborne Integrated Mapping System (AIMS), ISPRS Commission Symposium on Data Integration: systems and Techniques, 13-17 July, pp. 320-326, 1998.

[3] Hausdorff J. M., Ashkenazy Y., Peng C., Ivanov P., Stanley H., Goldberger A.: When human walking becomes random walking: fractal analysis and modeling of gait rhythm fluctuations, J. Physica, 302, pp. 138-147, 2001.

[4] Brand, T. J. and Phillips. R. E.: Foot-to-Foot Range Measurement as an Aid to Personal Navigation, Proceedings, ION AM, Albuquerque, NM, pp. 113-121, June 23-25, 2003.

[5] Cho, S. Y., Lee, K. W., and Lee, J. G.: A Personal Navigation System Using Low-Cost MEMS/GPS/Fluxgate, Proceedings, ION AM, Albuquerque, NM, pp. 122-127, June 23-25, 2003.

[6] Chau, T.: A review of analytical techniques for gait data. Part 1: fuzzy, statistical and fractal methods, J. Gait and Posture, 13, pp. 49-66, 2001a.

[7] Chau, T.: A review of analytical techniques for gait data. Part 2: neural networks and wavelet methods, J. Gait and Posture, 13, pp. 102-120, 2001b.

[8] Grejner-Brzezinska, D. A., Toth, C.K, and Yi, Y.: On Improving Navigation Accuracy of GPS/INS Systems, Photogrammetric Engineering & Remote Sensing, Vol. 71, 7-11 March, pp. 377-389, 2005.

[9] Yi, Y., Grejner-Brzezinska, D. A., and Toth, C. K.: Performance Analysis of a Low Cost MEMS IMU and GPS Integration, Proceedings, ION AM, pp. 1026-1036, June 26-29, 2005.